Volume 22, No 2 | International Journal of Radiation Research, April 2024

Accuracy of diffusion-weighted imaging in differentiation between medulloblastoma and ependymoma tumors

K.M. Abushab[1], S. Abu-Laila[2], M. Tabash[1], K. Quffa[1], A. Shaltout[2], Y.S. Alajerami[1*], H.H. Mansour[1], H. Beituni[3]

[1]Medical Imaging Department, Applied Medical Sciences Faculty, Al Azhar University-Gaza, Palestinian Territory
[2]Radiology Department, Al-Aqsa Hospital, Ministry of Health, Darussalam, Tanzania
[3]Medical Imaging Department, Health Sciences Faculty, HCT, UAE

► ***Original article***

Corresponding author:
Yasser S. Alajerami, Ph.D.,
E-mail:
yasser_ajr@hotmail.com

Received: May 2023
Final revised: September 2023
Accepted: September 2023

Int. J. Radiat. Res., April 2024; 22(2): 395-401

DOI: 10.61186/ijrr.22.2.395

Keywords: *Diffusion-weighted imaging, medulloblastoma, ependymoma.*

ABSTRACT

Background: To investigate the accuracy of diffusion-weighted imaging (DWI) in the differentiation between medulloblastoma and ependymoma tumors. ***Materials and Methods:*** A retrospectively analytical study was used. Eighty-nine patients with medulloblastoma and ependymoma tumors were included, as proved by the histopathological findings (2016–2019), and their ages ranged from 1 month to 15 years old. All DWI data were transferred through RadiAnt Dicom viewer and apparent diffusion coefficient (ADC) value calculations. Statistical analyses were conducted utilizing statistical software (MedCalc, version 19.0.4). ***Results:*** The value of ADCmean was the significant ADC value that distinguished medulloblastoma from ependymoma. The value of ADCmean was inversely proportional to tumor grades. The ADCmean value at the ependymoma tumor was 1.141±0.293 mm2/s, whereas the ADCmean value at medulloblastoma tumor was 0.661± 0.123 mm2/s. Spearman's correlation shows a significant negative correlation, and ADCmean (r = -0.72, P-value = 0.0001). The ADCmean has confirmed the highest diagnostic accuracy with an area under the curve (AUC) of 0.984 in cases in reference to histopathological findings as a gold standard and detects medulloblastomas and ependymomas tumors with sensitivity (96.92%), specificity (95.83%), PPV (98.4%,), NPV (92%) and accuracy (92.7%). There is a high level of agreement between the results of ADC value and histopathological findings, which is excellent agreement between the two tests as Kappa =0.915. ADCmean could serve as a base to distinguish medulloblastoma from ependymoma tumors with high accuracy. ***Conclusion:*** Using ADC map value to diagnose pediatric tumors could provide reliable and objective evidence for pre-operative differentiation.

INTRODUCTION

Brain tumors are one of the most common solid tumors in children and the cause of cancer-related mortality in children [1]. Brain tumors are mostly classified according to histogenesis principles, which allow for tumor categorization based on microscopic similarities to several postulated cells of origin and their presumed phases of differentiation [2]. Medulloblastoma is a common malignant brain tumor that occurs during childhood and accounts for 15-20% of pediatric brain tumors [3, 4]. The tumor usually occurs in the cerebellum and commonly invades the fourth ventricle in one-third of cases, developing metastases throughout the spinal cord [5]. The related symptoms are vague in complaints, and diagnosis is usually delayed. However, 70% to 80% of cases were diagnosed before metastasis, while 20% to 30% fall into higher-risk groups [6]. Ependymomas are infrequent neoplasms originating in the central nervous system (CNS). The World Health Organization (WHO) has histologically classified this condition into three classes (I, II, or III), with the degree of anaplasia determining the grading [7]. Glial tumors, which originate from ependymal cells that are specialized and line the ventricles of the brain and the central canal of the spinal cord, constitute a significant majority (about 80–90%) of intramedullary spinal cancers. Ependymoma occurs twice as frequently as astrocytomas [4, 8].

Computed tomography (CT) scans are valuable for detecting structural abnormalities and can provide relatively quick imaging results. However, CT scans involve the use of ionizing radiation, which poses a significant concern, especially in pediatric patients [9, 10]. Additionally, in cases of medulloblastoma and ependymoma, CT scans may be less preferable due to the limited soft tissue contrast compared to magnetic resonance imaging (MRI). Despite these advantages of MRI, pediatric posterior fossa tumors, including medulloblastoma and ependymoma, can be challenging to diagnose accurately using conventional MRI. However, the addition of diffusion-weighted imaging (DWI) can enhance the diagnostic process. DWI allows the evaluation of water diffusivity and quantifies the analysis of the average

[Downloaded from ijrr.com on 2026-11-22]

[DOI: 10.61186/ijrr.22.2.395]

diffusion rate in each voxel. Apparent diffusion coefficient (ADC) values obtained from DWI may increase the accuracy of pre-operative differentiation between medulloblastoma and ependymoma [11, 12].

Interpretation of ADC values may improve the diagnostic rate allow the correct identification of tumors in the majority of cases [13]. This study aimed to investigate the accuracy of DWI in distinguishing between medulloblastoma and ependymoma tumors, specifically in pediatric patients, and determining an optimal ADC cut-off value to differentiate between medulloblastoma and ependymoma tumors in pediatric posterior fossa tumors. Most previous studies have evaluated the use of DWI and ADC values in the diagnosis of pediatric brain tumors, while this study focuses specifically on the differentiation between medulloblastoma and ependymoma, which can be challenging on conventional MRI. Additionally, this study could be among the first to determine an optimal ADC threshold for discrimination between medulloblastoma and ependymoma in a pediatric population. It could allow more accurate pre-operative diagnosis and stratification of these tumors.

MATERIAL AND METHODS

Patient selection

A retrospectively analytical, cross-sectional study was used. Census sampling was applied to all cases with a registration profile in the targeted hospitals based on the Ministry of Health (MoH) registry. The total number of brain tumor cases was 205. The cases were obtained from the governmental oncology centers. Eighty-nine patients met the inclusion criteria and were included in the study. Patients aged one month to 15 years, of both genders, diagnosed with medulloblastoma or ependymoma with suitable solid tumor portions for ROI analysis were included. Patients were lacking complete registration files, DWI records, histopathological results, those with prior intracranial surgery, entirely cystic lesions, and follow-up cases.

All eighty-nine patients were diagnosed as posterior fossa tumor cases, specifically medulloblastoma and ependymoma, as proved by the histopathological findings (2016–2019), and their ages ranged from 1 month to 15 years old. All DWI data was transferred from the workstation to the personal computer through the RadiAnt Dicom viewer, and ADC value calculations were performed.

MRI data acquisition

MRI examinations were performed on a 1.5 T scanner (Philips-Intera) with a 16-channel body coil. The imaging sequence for DWI was a multi-section echo planner (EPI) sequence (TR/TE/NEX: 6000/102 ms/1; b = 0, 1000 s/mm^2). DWI was acquired prior to the administration of contrast media. The diffusion gradients were applied sequentially in three orthogonal directions (X, Y, and Z directions). Slice sections of 5 mm thickness, a slice gap of 1 mm, a FOV of 240–260 mm, and a matrix of 128 × 256 were used for all images. The total acquisition time was 2.08 minutes. For each patient, the enhancing solid portion of the lesion was identified on post-contrast T1-weighted images, matching the slice position of the ADC map.

Quantitative analysis

All measurements were carried out utilizing the RadiAnt DICOM viewer (version 2020.1), available at https://www.radiantviewer.com/. Three regions of interest (ROIs) of 30 mm^2 were drawn on the solid part of the tumor at three consecutive slice positions of the tumor and were placed without overlapping. A neuroradiologist with 10–15 years of clinical experience verified the placement of ROIs in all cases. Every value is computed automatically and given in terms of 10^{-3} mm^2/s.

The initial region of interest (ROI) was positioned over the consistently enhancing regions within the tumor, with the exclusion of necrotic or hemorrhagic regions. Subsequently, two more ROIs were situated in different sections with homogeneous enhancement. This process resulted in a total of three ROIs from the lesions, which were then segmented and averaged to establish the average ADC value for the tumor. In the case of contrast-enhanced tumor patients, the ROI was positioned at the location of the enhanced lesions observed on the contrast-enhanced T1-weighted MRI.

Statistical analysis

Statistical analyses were conducted utilizing statistical software (MedCalc, version 19.0.4). The initial step involved creating the data entry foundation and encoding variables, followed by the actual input of data. During the analysis phase, the data underwent cleaning and management for the variables of interest. Descriptive analysis, encompassing graphical representations and frequency tables, was employed to depict the primary characteristics of the dataset. A *t-test* was used to examine the differences in ADC values between normal tissue and tumors. The receiver operating characteristic (ROC) curve and AUR were used to measure the sensitivity and specificity of DWI in the diagnosis of brain tumors, considering histopathology as a gold standard. Agreement (KAPPA test) was used to correlate the finding of the ADC value with histopathology. The confidence interval considered is 95%, and a p-value < 0.05 is statistically significant.

[Downloaded from ijrr.com on 2026-11-22]

[DOI: 10.61186/ijrr.22.2.395]

RESULTS

The results revealed that 58 (65.2%) cases were males and 31 (34.8%) were females. Half were six years old or less, with a mean age of 6.09±3.35 years. The majority of the tumors, 77 (86.5%), were located in the posterior fossa at the level of the 4th ventricle, and 8 (9%) were located at the supratentorial intra-axial. The rest are located at other locations, as mentioned in table 1. In histopathology results, the majority of medulloblastoma constitutes 65 (73%) of the brain tumors, while ependymoma constitutes 24 (27%) of the tumors. According to histopathology findings, 24(27%) of the cases were diagnosed or confirmed as epidymoma, which was classified as grade II or III, according to the WHO. In comparison, 65(73%) were diagnosed or confirmed as medulloblastoma and classified as grade IV.

Table 1. Patient characteristics based on demographic factors and tumor classifications.

Variable n=89	No.	%
Gender		
Male	58	65.2
Female	31	34.8
Age		
Less than 6 years old	46	51.7
More than 6 years old	43	48.3
Tumor location		
Posterior Fossa /4th ventricle	77	86.6
Supratentorial intra-axial	8	9.0
Supratentorial intra-ventricular	1	1.1
Supratentorial intra-axial	2	2.2
Posterior Fossa	1	1.1
Tumor type in histopathology		
Ependymoma	24	27
Medulloblastoma	65	73
Tumor grade		
2.00	13	14.6
3.00	11	12.4
4.00	65	73.0

Table 2 shows the ADC values of 89 patients diagnosed with either ependymoma or medulloblastoma based on histopathological results. Twenty-four cases were defined as ependymoma, and the mean value of ADC at the tumor was 1.141±0.293 mm^2/s. Based on WHO classification, 13 cases were grade II with an ADC_{mean} value of 1.154±0.294 mm^2/s, and 11 cases were grade three with an ADC_{mean} value of 1.126±0.306 mm^2/s. On the other hand, sixty-five patients diagnosed with medulloblastoma (grade IV) have an ADC_{mean} value of 0.661± 0.123 mm^2/s.

Table 2. ADC values of ependymoma and medulloblastoma tumors.

Variable (n=89)	N	Mean (SD) $ADC_{mean} \times 10^{-3}$ mm^2/s	Male/ Female
Ependymoma	24	1.141± 0.293	15/9
Grade II	13	1.154± .294	8/5
Grade III	11	1.126± .306	7/4
Medulloblastoma (VI)	65	0.661± 0.123	43/22

ADC mean: Apparent Diffusion Coefficient mean

Differences in ADC Values between studied brain tumors

An independent *t-test* was used to compare the mean ADC value at both tumor sites with normal brain tissue (table 3). In the assessment of ADC values in normal brain tissue, we observed that ependymoma exhibited a slightly higher mean ADC value (ADC_{mean} = 0.800 ± 0.051), whereas medulloblastoma showed a slightly lower mean ADC value (ADC_{mean} = 0.791 ± 0.055). However, there is no statistically significant difference in ADC values between these two tumor types within normal brain tissue (P = 0.471). Consequently, this suggests that both ependymoma and medulloblastoma may manifest relatively similar ADC characteristics in the surrounding healthy brain tissue. In contrast, the analysis of ADC values within the tumor regions revealed a striking difference between ependymoma and medulloblastoma. Ependymoma exhibited a notably higher mean ADC value (ADC_{mean} = 1.141 ± 0.393), while medulloblastoma displayed a substantially lower mean ADC value (ADC_{mean} = 0.661 ± 0.123). The t-statistic indicates a highly significant distinction in ADC values within tumor regions between the two tumor types (t = 10.88, P <0.001).

Table 3. Differences in ADC normal and ADC values at tumor between brain tumors.

Variable n=89	N	Mean	SD	t	sig
ADC normal					
Ependymoma	24	0.800	0.051	0.724	0.471
Medulloblastoma	65	0.791	0.055		
ADC mean at tumor					
Ependymoma	24	1.141	0.393	10.88	< 0.001*
Medulloblastoma	65	0.661	0.123		

Correlation between the ADC_{mean} and histopathology findings

A Spearman-correlation was conducted test was conducted to determine the correlation between ADC_{mean} and grades of the tumor as reported by histopathology results (figure 1). Indices of Spearman correlation show a significant negative correlation between both medulloblastomas, and ependymomas and ADC value at the significance level (r = -0.7196, P-value = 0.0001).

AUR Curve and ADC_{mean} cut-off Value in ADC_{mean} at the tumor

The area under the ROC curve of the ADC tumor diagnostic test in DWI-MRI is demonstrated in table 4 and figure 2. The ROC curve showed that the area under the curve of the diagnostic rate of tumors by the ADC_{mean} MRI scan was (0.984). The ADC value measurements can detect medulloblastomas and ependymoma tumors with sensitivity (96.92%), specificity (95.83%), PPV (98.4%), NPV (92%), and accuracy (92.7%). Based on the cellularity of the tumor, the cut-off value that has the highest sensitivity and specificity for the diagnostic test and can distinguish between medulloblastomas and

[Downloaded from ijrr.com on 2026-11-22]

[DOI: 10.61186/ijrr.22.2.395]

ependymomas tumors is equal to $0.889\times10^{-3}mm^2/s$.

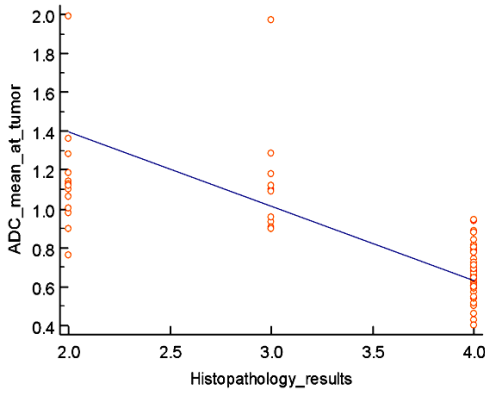


Figure 1. Spearman's correlation between histopathology results and the ADCmean value at the tumor. The results reveal a strong negative correlation (-0.7196) between ADC mean values and tumor grades for both medulloblastomas and ependymomas.

Table 4. Optimal cut-off value to discriminate Medulloblastoma from ependymoma tumors.

Comparison		AUC (95% CI)	Optimal ADC cut-off value	Sensitivity	Specificity	+PV	-PV	Accuracy
ADC_{mean}	M vs. E	0.984 0.931-0.999	≤0.889	96.92	95.83	98.4	92.0	0.9276

ADC mean: Apparent Diffusion Coefficient mean.
M: Medulloblastomas. E: Ependymoma

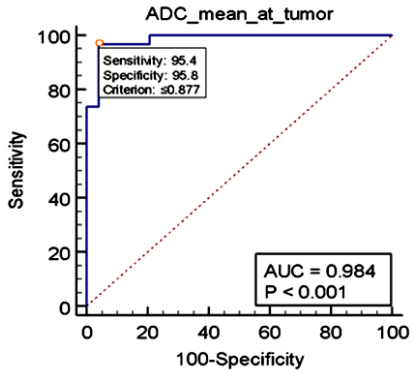


Figure 2. ROC curve of ADCmean at the tumor: The ROC curve illustrates the diagnostic performance of ADC mean MRI scans in distinguishing between medulloblastomas and ependymoma tumors. The area under the ROC curve (AUC) is calculated at 0.984, indicating a high discriminatory ability of ADC values in tumor diagnosis.

Agreement between ADC_{mean} and histopathology findings

The study revealed that out of 89 cases diagnosed by ADCmean and histopathological findings, 23 cases were recognized as ependymoma and two as medulloblastoma. However, the procedures are not agreed upon in three cases (table 5). Two cases were recognized as Ependymoma at $ADC_{mean,}$ while in histopathology, it was recognized as Medulloblastoma. Also, one case was recognized as Medulloblastoma at ADC_{mean} and Ependymoma in histopathological findings. There is consistency between the results of the ADC_{mean} and histopathology finding as revealed by excellent agreement between the two tests as Kappa = 0.915 with a statistically significant difference (P < 0.001).

Table 5. Agreement between ADCmean and histopathology findings.

Variable (*n=89*)		Histopathology		Kappa	*P*-value
		Ependymoma	Medulloblastoma		
ADC_{mean}	Ependymoma	23	2	0.915	<.001*
	Medulloblastoma	1	63		

Representative cases are shown in figure 3 and 4.

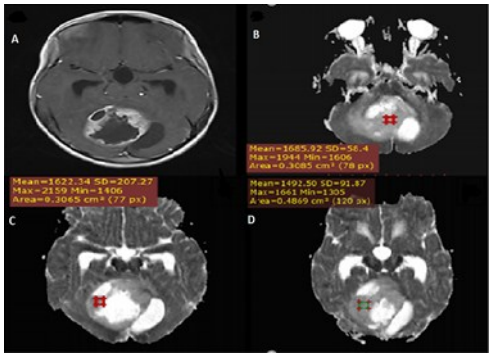


Figure 3. presents the case of an 11-year-old female patient diagnosed with medulloblastoma. The diagnosis was established based on routine sequences and post-contrast axial T1-weighted imaging (T1WI) **(A)**. In this analysis, three distinct regions of interest (ROI) were strategically positioned away from areas displaying necrosis or hemorrhage within the tumor. These ROIs were carefully selected on three consecutive slices of the apparent diffusion coefficient (ADC) map **(B, C, and D)**. The RadiAnt DICOM viewer was utilized to perform an automatic calculation of the mean, minimum, and maximum signal intensity values within the ADC map.

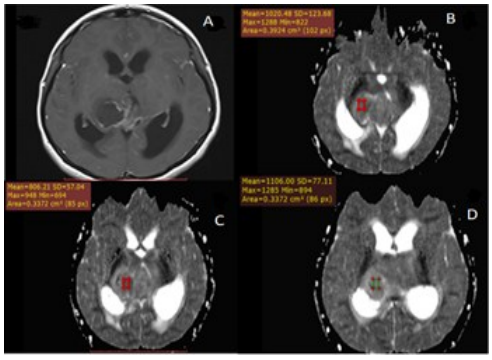


Figure 3. presents the case of an 11-year-old female patient diagnosed with medulloblastoma. The diagnosis was established based on routine sequences and post-contrast axial T1-weighted imaging (T1WI) **(A)**. In this analysis, three distinct regions of interest (ROI) were strategically positioned away from areas displaying necrosis or hemorrhage within the tumor. These ROIs were carefully selected on three consecutive slices of the apparent diffusion coefficient (ADC) map **(B, C, and D)**. The RadiAnt DICOM viewer was utilized to perform an automatic calculation of the mean, minimum, and maximum signal intensity values within the ADC map.

DISCUSSION

The study was considered to explore the accuracy of DWI in distinguishing between medulloblastoma

[Downloaded from ijrr.com on 2026-11-22]

[DOI: 10.61186/ijrr.22.2.395]

and ependymoma tumors. This discrimination was based on histological grade findings and conducted utilizing 1.5 Tesla MRI systems. DWI and its ADC map are widely used in brain tumor detection; they provide image contrast based on water molecular diffusion characteristics in brain tumors [14]. It shows the random motions of water molecules that are influenced by many factors, including molecular type, tissue temperature, and diffusion occurring in the microenvironment [15]. The ADC value determines the absolute measurement of the diffusion amount. The value of ADC histograms usually indicates limited diffusion with low ADC values, while high ADC values indicate an increase in water diffusion [16].

These results confirmed that ADC value decreased when the grade of tumor increased, which is consistent with Yamasaki *et al.*'s finding that a significant negative correlation existed between ADC and tumors of WHO grades II–IV (grade II vs. grades III and IV) [17]. In addition, Guvain *et al.* reported that ADC in gliomas, germ cell tumors, and ependymomas is 1.22 ± 0.09 × 10^{-3} mm^2/s [18]. Rumboldt *et al.* studied posterior fossa tumors in 32 patients and measured ADC values. ADC values were significantly higher in ependymomas (1.10–0.11× 10^{-3} mm^2/s) (P =0.0003) than in medulloblastomas (0.66–0.15× 10^{-3} mm^2/s) (P = 0.0001) [19]. However, the ADC values obtained for ependymoma and medulloblastoma agreed with the grade of the tumor [20].

DWI plays a crucial role in distinguishing between tumor invasions from normal brain tissue or peri-focal brain edema. This differentiation is pivotal as it reduces the inherent risks associated with the biopsy of various brain tumor lesions [21]. The measurement of ADC values yields valuable insights into distinguishing between different pathological conditions, including edema and specific lesion types such as tumors, cysts, hamartomas, leukodystrophies, and infections [22].

Furthermore, the Spearman correlation analysis in our study demonstrates a noteworthy negative correlation (r = -0.7196, P-value = 0.0001) between ADC values and both medulloblastomas and ependymomas. There is evidence regarding the correlation between ADC, particularly ADC_{mean}, and cellularity in different tumors with a moderate inverse correlation and cellularity [23, 24]. It is noteworthy that a recurrent finding in the literature is the inverse correlation between cell densities and ADC values, a trend that is particularly prominent in pediatric cerebellar tumors [16, 25, 26].

In recent years, DWI-MRI has emerged as a powerful and effective diagnostic tool for brain tumor detection [27]. Tissues with a high cellular density tend to exhibit a more gradual attenuation slope in DWI with corresponding ADC values [28]. Medulloblastoma tumors are characterized by their histological features of high cellularity and a pattern of densely packed small cells, often accompanied by small areas of necrosis. These traits result in lower or diminished ADC values in medulloblastoma cases [29]. This phenomenon is consistent with the strong negative correlation observed between ADC values and tumor cellularity in patients, mainly those with brain tumors (r = −0.57; CI = −0.62, −0.52) [30].

A study conducted by Woodhams *et al.* further emphasized this relationship, revealing a strong inverse correlation between ADC and cell count and proposing the ADC value as a reliable imaging tool to estimate tumor cellularity [31]. In contrast, there was a moderate negative correlation between WHO-grade and ADC_{mean} (Spearman's Rank; ADC_{mean}: -0.606; 95% CI (-0.773 to -0.384); ADC_{min}: 95% CI (-0.759 to -0.353), suggesting that ADC values may not be as closely tied to tumor grading as they are to cellularity [32]. These findings collectively underscore the potential of DWI-MRI and ADC measurements in non-invasively assessing cellular density and, to some extent, tumor grading in brain tumors, thereby aiding clinicians in making informed decisions regarding patient management.

The study results revealed that the value of ADC_{mean} can effectively differentiate medulloblastomas from ependymomas with a high degree of sensitivity, specificity, and accuracy based on the cut-off ADC_{mean} point. The results were consistent with a study by Porto *et al.*, where they identified a cut-off value of 1.0 × 10^{-3} mm^2/s for average ADC values, successfully distinguishing between low and high-grade pediatric brain tumors [13]. Furthermore, good accuracy with mean ADC values of ≥1.4×10^{-3} mm^2/s accurately differentiated pilocytic astrocytomas from ependymomas, exhibiting a sensitivity of 0.75 and a specificity of 0.86. In comparison, when the ADC_{mean} values were <0.85×10^{-3} mm^2/s, they effectively distinguished embryonal tumors from ependymomas with a sensitivity of 0.82 and a specificity of 0.67 [33].

The current study showed higher level of agreement between the results of ADC_{mean} and histopathological findings, indicating the potential for valuable prediction of a histological grade and effective discrimination between medulloblastomas and ependymomas (kappa value = 0.915). This substantial agreement underscores the clinical utility of ADC_{mean} values in providing accurate insights into tumor characterization and grading.

The observed differentiation in diffusion characteristics between ependymoma and medulloblastoma, with no overlap between the two, aligns with the findings of a study conducted by Yamasaki et al., which reported that ADC values were 100% accurate in distinguishing between primitive neuroectodermal tumors and ependymomas [17]. Similarly, our results are consistent with a study performed by Rumboldt *et al.*, which confirmed a significant difference between the ADC value of medulloblastoma and the ADC value of ependymoma

[Downloaded from ijrr.com on 2026-11-22]

[DOI: 10.61186/ijrr.22.2.395]

[19]. Additionally, a retrospective study identified that ADC value thresholds successfully distinguished high -grade medulloblastoma from low-grade tumors or others in 91% of cases, enabling accurate lesion identification [13].

CONCLUSION

The ADC_{mean} values exhibited a strong correlation with the grades of medulloblastomas and ependymomas and could serve as a base to differentiate medulloblastoma from ependymoma tumors with a high degree of accuracy. According to the results of the KAPPA analysis, ADC_{mean} attained a high agreement with histopathological findings, as long it had a chance to advance perception as a simple and effective implement in distinguishing between medulloblastoma and ependymoma tumors. Thus, using the ADC map value to diagnose pediatric tumors, medulloblastoma, and ependymoma could provide reliable and objective evidence for pre-operative differentiation.

***Ethical and administrative considerations*:** Approval was obtained from all participants, including the ethical committee of the Ministry of Health in the Gaza Strip (Helsinki committee No. PHRC/HC/560/19), before the start of the study.

***Funding*:** This research received no specific grant from any funding agency in the public, commercial, or not-for-profit sectors.

***Data Availability*:** The data supporting the study's findings are available from the corresponding author upon reasonable request.

***Conflicts of interest*:** The authors declare that they have no conflicts of interest.

***Authors' contributions*:** Abushab KM, Abu-Laila SW, Mansour HH, and Alajerami YS participated in idea formation and data gathering. Tabash MI, Quffa KM, Shaltout A, and Beituni H participated in data analysis and interpretation. All contributors participated in manuscript drafting, revising, and approval of the manuscript and agreed with study publication.

REFERENCES

1. Partap S and Monje M (2020) Pediatric brain tumors. *CONTINUUM: Lifelong Learning in Neurology, **26**(6): 1553-1583*.
2. Louis DN, Perry A, Reifenberger G, *et al.* (2016) The 2016 World Health Organization classification of tumors of the central nervous system: a summary. *Acta neuropathologica*, ***131***(6): 803-820
3. Kumar L, Deepa SF, Moinca I, *et al.* (2015) Medulloblastoma: A common pediatric tumor: Prognostic factors and predictors of outcome. *Asian Journal of Neurosurgery, **10**(01): 50-50*.
4. Ostrom, QT, De Blank PM, Kruchko C, *et al.* (2014) Alex's lemonade stand Foundation infant and childhood primary brain and central nervous system tumors diagnosed in the United States in 2007–2011. *Neuro-Oncology, **16**(10): x1-x36*.
5. Kline CN, Packer RJ, Hwang EI, *et al.* (2017) Case-based review: Pediatric medulloblastoma. *Neuro-Oncology Practice*, ***4***(3*): 138-150*.
6. Quinlan A, Rizzolo D (2017). Understanding medulloblastoma. *JAAPA, **30**(10): 30-36*.
7. Cachia D, Johnson DR, Kaufmann TJ, *et al.* (2018) Case-based review: Ependymomas in adults. *Neuro-Oncology Practice, **5**(3): 142-153*.
8. Choi J, Chang K, Yu IK, *et al.* (2002). Intracranial and spinal Ependymomas: Review of MR images in 61 patients. *Korean Journal of Radiology, 3(4): 219*.
9. Mansour HH, Alajerami YS, Foster T (2021) Estimation of radiation doses and lifetime attributable risk of radiation-induced cancer from a single coronary artery bypass graft computed tomography angiography. *Electron J Gen Med, **18**(6): em317.*
10. Abushab KM, Mansour HH, Alajerami YS (2021) Assessment of patient radiation dose in dual-phase abdominopelvic computed tomography. *Int J Radiat Res, **20**(4): 879-882*.
11. Porto L, Jurcoane A, Schwabe D, Kieslich M, Hattingen E (2013). Differentiation between high and low grade tumours in paediatric patients by using apparent diffusion coefficients. *European Journal of Paediatric Neurology, **17**(3): 302-307*.
12. Hygino da Cruz LC, Vieira IG, Domingues RC (2011) Diffusion MR imaging: An important tool in the assessment of brain tumors. *Neuroimaging Clinics of North America, **21**(1): 27-49*.
13. Pierce T, Kranz PG, Roth C, *et al.* (2014) Use of apparent diffusion coefficient values for diagnosis of pediatric posterior fossa tumors. *The Neuroradiology Journal, **27**(2): 233-244*.
14. Huisman T (2010) Diffusion-weighted and diffusion tensor imaging of the brain, made easy. *Cancer Imaging, **10**(1A): S163-S171*.
15. Huisman TA (2003) Diffusion-weighted imaging: Basic concepts and application in cerebral stroke and head trauma. *European Radiology, **13**(10): 2283-2297*.
16. Eidel O, Neumann J, Burth S, *et al.* (2016) Automatic analysis of Cellularity in glioblastoma and correlation with ADC using trajectory analysis and automatic nuclei counting. *Plos One*, ***11**(7): e0160250*.
17. Yamasaki F, Kurisu K, Satoh K, *et al.* (2005) Apparent diffusion coefficient of human brain tumors at MR imaging. *Radiology, **235**(3): 985-991*.
18. Gauvain KM, McKinstry RC, Mukherjee P, *et al.* (2001) Evaluating pediatric brain tumor Cellularity with diffusion-tensor imaging. *American Journal of Roentgenology, **177**(2): 449-454*.
19. Rumboldt Z, Camacho DL, Lake D, *et al.* (2006) Apparent diffusion coefficients for differentiation of cerebellar tumors in children. *AJNR Am J Neuroradiol, **27**(6): 1362-1369*.
20. Jaremko J, Jans L, Coleman L, Ditchfield M (2010) Value and limitations of diffusion-weighted imaging in grading and diagnosis of pediatric posterior fossa tumors: Fig 1. *American Journal of Neuroradiology, **31**(9): 1613-1616*.
21. Stadnik TW, Demaerel P, Luypaert RR, *et al.* (2003) Imaging tutorial: Differential diagnosis of bright lesions on diffusion-weighted MR images. *RadioGraphics, **23**(1): e7-e7*.
22. Sener RN (2001) Diffusion MRI: Apparent diffusion coefficient (ADC) values in the normal brain and a classification of brain disorders based on ADC values. *Computerized Medical Imaging and Graphics, **25**(4): 299-326*.
23. Surov A, Meyer HJ, Wienke A (2017) Correlation between minimum apparent diffusion coefficient (ADCmin) and tumor cellularity: A meta-analysis. *Anticancer Research, **37**(7): 3807-3810*.
24. Zong RL, Geng L, Wang X, Xie D (2019) Diagnostic performance of apparent diffusion coefficient for prediction of grading of pancreatic neuroendocrine tumors. *Pancreas, **48**(2): 151-160*.
25. Barajas R, Rubenstein J, Chang J*, et al.* (2009) Diffusion-weighted MR imaging derived apparent diffusion coefficient is predictive of clinical outcome in primary central nervous system lymphoma. *American Journal of Neuroradiology, **31**(1): 60-66*.
26. Wu X, Pertovaara H, Dastidar P, *et al.* (2013) ADC measurements in diffuse large B-cell lymphoma and follicular lymphoma: A DWI and cellularity study. *European Journal of Radiology, **82**(4): e158-e164*.
27. Mustafa WF,Abbas M, Elsorougy L (2020) Role of diffusion-weighted imaging in differentiation between posterior fossa brain tumors. *The Egyptian Journal of Neurology, Psychiatry and Neurosurgery, **56**(1): 1-8*.
28. Koh DM and Collins DJ (2007) Diffusion-weighted MRI in the body: Applications and challenges in oncology. *American Journal of Roentgenology, **188**(6): 1622-1635*.
29. Ellison D (2002) Classifying the Medulloblastoma: Insights from morphology and molecular genetics. *Neuropathology and Applied Neurobiology, **28**(4): 257-282*.
30. Chen Z, Ma L, Lou X, Zhou Z (2010) Diagnostic value of minimum

[Downloaded from ijrr.com on 2026-11-22]

[DOI: 10.61186/ijrr.22.2.395]

apparent diffusion coefficient values in prediction of neuroepithelial tumor grading. *Journal of Magnetic Resonance Imaging,* ***31****(6): 1331-1338*.

31. Woodhams R, Kakita S, Hata H, *et al.* (2009) Diffusion-weighted imaging of Mucinous carcinoma of the breast: Evaluation of apparent diffusion coefficient and signal intensity in correlation with histologic findings. *American Journal of Roentgenology,* ***193****(1): 260-266*.
32. Mebis W, Snoeckx A, Corthouts B, *et al.* (2020) Correlation between apparent diffusion coefficient value on MRI and Histopathologic WHO grades of neuroendocrine tumors. *Journal of the Belgian Society of Radiology,* ***104****(1).*
33. Koral K, Alford R, Choudhury N, *et al.* (2014) Applicability of apparent diffusion coefficient ratios in preoperative diagnosis of common pediatric cerebellar tumors across two institutions. *Neuroradiology,* ***56****(9): 781-788*.

[Downloaded from ijrr.com on 2026-11-22]

[DOI: 10.61186/ijrr.22.2.395]

[DOI: 10.61186/ijrr.22.2.395] [Downloaded from ijrr.com on 2026-11-22]